Investigation of the Noise Performance of Double-Gate MOSFETs by Deterministic Simulation of the Boltzmann Equation

Sung-Min Hong and Christoph Jungemann
EIT4, Bundeswehr University, 85577 Neubiberg, Germany
Email: hi2ska2@gmail.com, Jungemann@ieee.org

***Abstract*—Noise performance of a double-gate MOSFET is investigated by deterministic simulation of the Boltzmann equation. The fully-coupled scheme of the Boltzmann equation and Poisson equation enables both, rapid convergence of the Newton-Raphson method and noise analysis. In contrast to Monte Carlo noise simulation, it is possible to determine the spatial origin of the terminal current noise. It is confirmed that the larger part of the terminal current noise stems from the source side.**

I. Introduction

The double-gate (DG) MOSFET (or FinFET) has attracted much attention in the past years. Since noise could be a limiting factor of the DG MOSFET for both analog and digital applications, an accurate method to evaluate the noise performance of this device is required. In this work, the noise performance of DG MOSFETs is investigated by using a deterministic Boltzmann equation solver.

II. Model

A Boltzmann solver based on the spherical harmonics expansion of the electron distribution function in the momentum-space [1] has been developed. Electron transport is based on the nonparabolic six valley band structure and phonon mechanisms developed by the Modena group [2]. In this work, the quantization of carrier motion perpendicular to the interface is not taken into account. In order to account for inversion-layer transport, additional scattering mechanisms are included in the simulation [3], and the parameters for those scattering processes are matched to the Lombardi mobility model [4].

Numerical performance of the Boltzmann solver heavily depends on the discretization scheme. In this work, the so-called "H-transformation," where balance equations derived from the Boltzmann equation by expanding with spherical harmonics are formulated in the total energy space, is employed in order to obtain a stable discretization scheme [1]. Since the resultant equations do not contain the partial derivative with respect to the total energy, it can be easily stabilized by introducing the direct/adjoint (dual) grid scheme [5]. One obvious strength of the H-transformation over the discretization scheme based on the kinetic energy is that the free-streaming operator can be treated correctly even in the ballistic limit.

However, the stable scheme becomes possible only at a certain cost. From its definition, the total energy grid must be aligned with the electrostatic potential. We consider the detailed dependence of the density-of-states, the electron velocity, and the scattering rate on the electric potential. Using this fully-coupled scheme, rapid convergence can be obtained by the Newton-Raphson method, in contrast to previous Gummel-type attempts [1], [3].

For the small-signal Jacobian matrix, the linearized Boltzmann equation is built upon the steady-state total energy [6]. As a result, the fluctuating electric potential introduces additional coupling between two discretized nodes with different total energy. The Green's function for the terminal noise current can be obtained by a solution of the corresponding adjoint system of equations. Noise simulation is performed in the way described in [7].

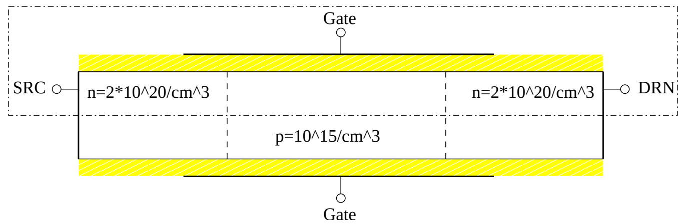

Fig. 1. Structure of the simulated double-gate (DG) NMOSFET.

III. Simulation Results

In Fig. 1 the structure of the simulated DG MOSFET [8] is shown. The length of the metal gate is 70 nm. The oxide thickness is 1.3 nm and the metallurgical channel length 50 nm. The body of the DG MOSFET is 20 nm thick. A uniform energy grid with 5 meV spacing is adopted in the following simulations. The maximum order of spherical harmonics is 3.

Fig. 2 shows the zeroth order component (an average over the solid angle) of the electron distribution function for the valleys for which the longitudinal mass in $\boldsymbol{k}$-space is parallel to the x-axis. The value at the interface is presented. Note that the "energy" in the figure represents the total energy. The distribution function can be simulated over several orders of magnitude without problems. The distribution function at the drain contact consists of two parts, a large number of electrons close to equilibrium at lower energy and the injected electrons from the source contact at higher energy. Also near the drain

978-1-4244-3947-8/09/$25.00 ©2009 IEEE

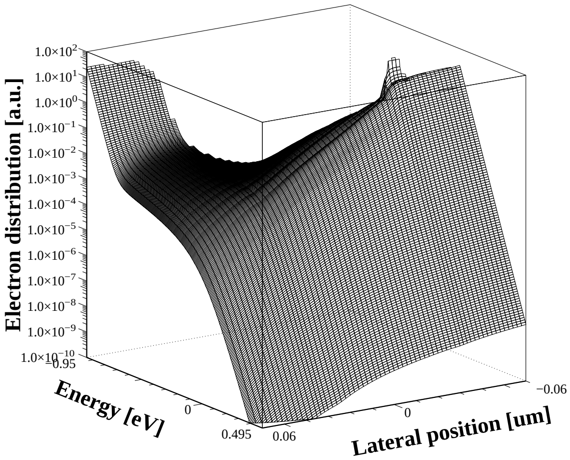

Fig. 2. Electron distribution function at V_{GS} = 0.9 V and V_{DS} = 0.9 V. The value at the interface is shown.

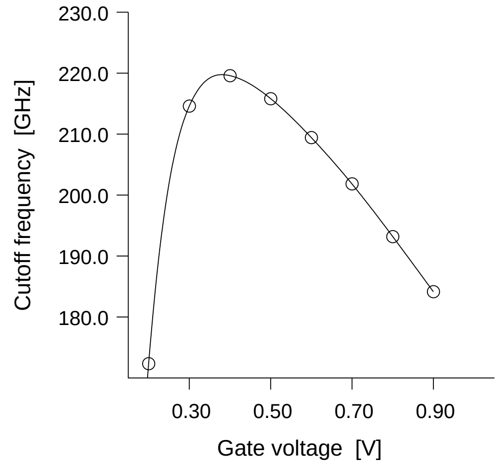

Fig. 4. Cutoff frequency at V_{DS} = 0.9 V. The peak cutoff frequency is about 220 GHz.

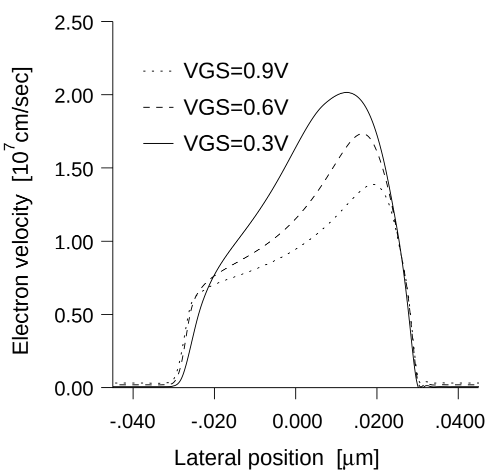

Fig. 3. Longitudinal electron velocity averaged perpendicular to the channel direction at V_{DS} = 0.9 V.

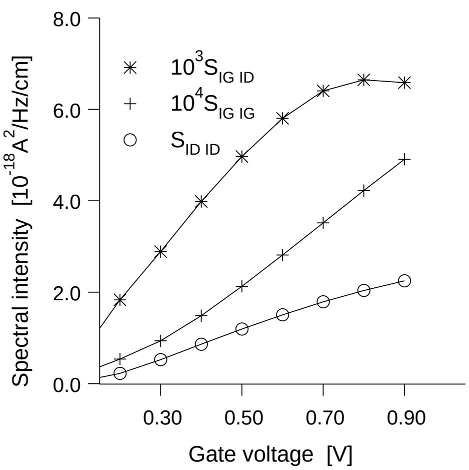

Fig. 5. Spectral intensities of the terminal current noise as a function of V_{GS} at V_{DS} = 0.9 V and 10 GHz. Absolute value is shown for $S_{I_G I_D}$.

end of the channel, energy dissipation by the dominant phonon mode is clearly visible.

Fig. 3 shows the longitudinal electron velocity profile. The lateral position of the middle of the channel is denoted as zero. Velocity overshoot, where the peak velocity is twice as large as the saturation velocity of silicon, is observed.

Since small-signal analysis is available, Y-parameters can be calculated in a straightforward manner, and hence the small-signal current gain. Fig. 4 shows the cutoff frequency extrapolated from the small-signal current gain at 10 GHz as a function of V_{GS}. The peak cutoff frequency is about 220 GHz.

Fig. 5 shows the spectral intensities of the terminal current noise as a function of V_{GS} at 10 GHz. The absolute value is shown for $S_{I_G I_D}$. $S_{I_G I_G}$ and $S_{I_G I_D}$, which are a few orders of magnitude smaller than $S_{I_D I_D}$, can be evaluated without numerical problems. Fig. 6 shows the spectral intensity of the drain current noise as a function of V_{DS} at 10 GHz. It increses monotonically, when V_{DS} increases. This behavior significantly deviates from the one predicted in the long-channel limit [9].

There have been many discussions about the contribution of hot carriers to the terminal current noise (e.g. [10]). Although by HD simulations [8] it was shown that the contribution from the source side is the dominant part in the drain noise, the confirmation with a Boltzmann equation solver is still lacking. Since the transfer functions from the local noise source to the observed output variable are available, it is possible to determine the spatial origin of the terminal current noise.

Fig. 7 shows the zeroth order component of the drain current Green's function for two different energies. For the low energy the Green's function is clearly determined by the channel barrier. On the other hand, for the high energy the transition region of the Green's function broadens. Even for electrons

978-1-4244-3947-8/09/$25.00 ©2009 IEEE

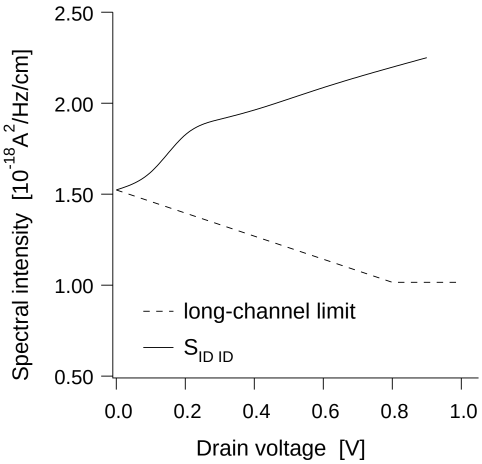

Fig. 6. Spectral intensity of the drain current noise as a function of V_{DS} at V_{GS} = 0.9 V and 10 GHz. The model value in the long-channel limit [9] is also shown for comparison.

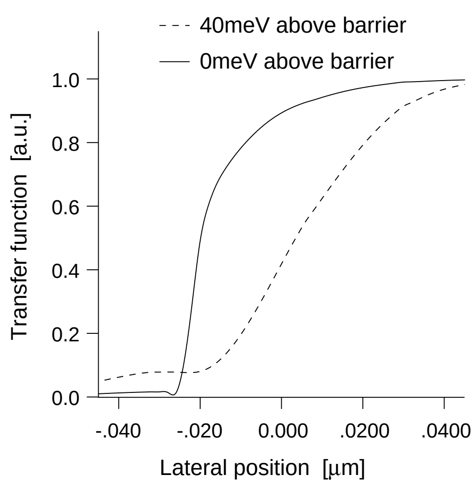

Fig. 7. Drain current Green's function for two different energies above the channel barrier at V_{GS} = 0.3 V, V_{DS} = 0.9 V, and 10 GHz. The real part at the interface is shown.

injected at the source region, there remains a small probability (about 8 %) to overcome the barrier and eventually to arrive the drain contact.

Figs. 8 and 9 show the spatial origin of the drain current noise and gate current noise, respectively. The larger part of the terminal current noise stems from the source side. This information is not available from the Monte Carlo method. Peaks around the metallurgical junctions are due to abrupt changes in the doping profile.

Since both, the Y-parameters and the spectral intensities of the terminal currents are available, it is straightforward to extract useful circuit parameters. Fig. 10 shows α and β parameters defined as [11]

$$\alpha = \frac{S_{I_D I_D}}{4k_B T|Y_{21}|},$$

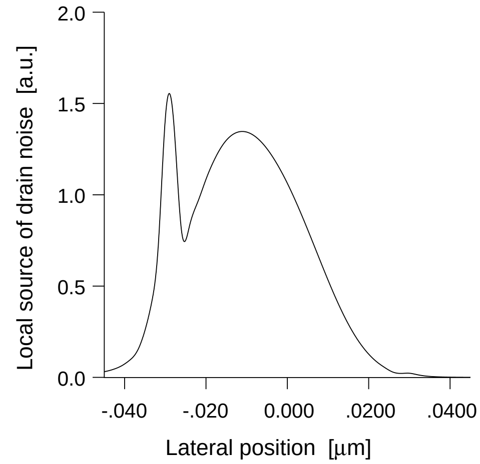

Fig. 8. Local contribution to the drain current noise integrated perpendicular to the channel direction at V_{GS} = 0.9 V, V_{DS} = 0.9 V, and 10 GHz.

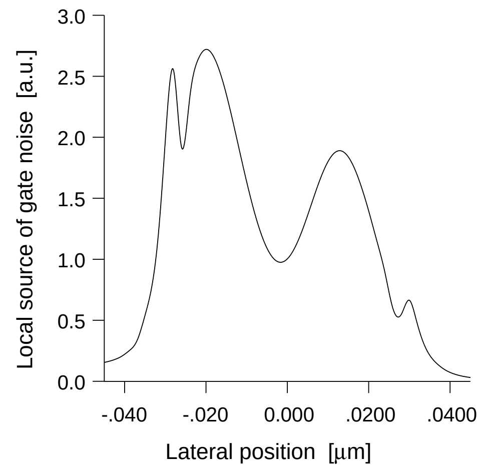

Fig. 9. Local contribution to the gate current noise integrated perpendicular to the channel direction at V_{GS} = 0.9 V, V_{DS} = 0.9 V, and 10 GHz.

$$\beta = \frac{S_{I_G I_G}|Y_{21}|}{4k_B T|Y_{11}|^2},$$

respectively.

Another quantity of interest is the correlation factor of the gate/drain current noise,

$$c = \frac{S_{I_G I_D}}{\sqrt{S_{I_G I_G} S_{I_D I_D}}}.$$

In the long channel limit [11], its imaginary part is about 0.4. The gate/drain correlation factor is shown in Fig. 11.

Since the cutoff frequency is as high as 220 GHz, the minimum noise figure of the device-under-simulation can be very low. The minimum noise figure is shown in Fig. 12. At 10 GHz, the minimum noise figure for V_{GS} = 0.3 V and V_{DS} = 0.9 V is as low as 0.1 dB.

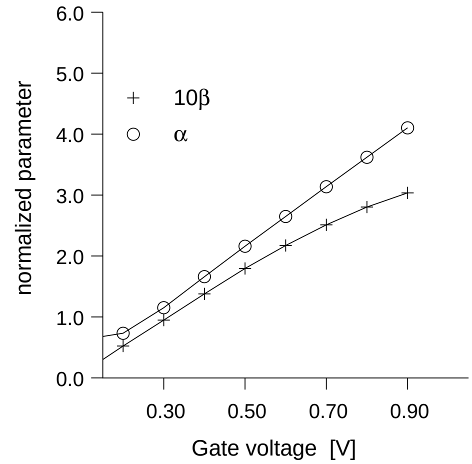

Fig. 10. Results for α and β as a function of V_{GS} at V_{DS} = 0.9 V and 10 GHz.

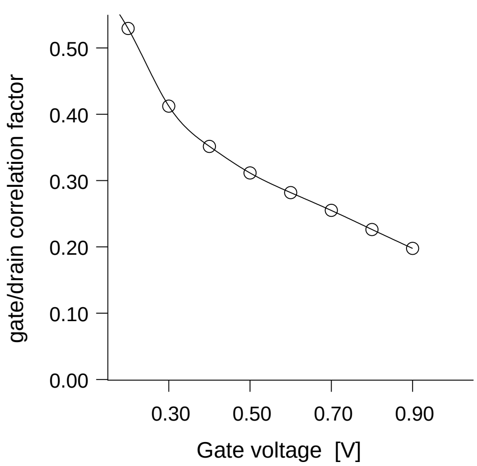

Fig. 11. Imaginary part of the gate/drain correlation factor as a function of V_{GS} at V_{DS} = 0.9 V and 10 GHz.

IV. Conclusion

In conclusion, we have implemented a deterministic Boltzmann solver based on the H-transformation. In contrast to the previous attempts, the fluctuations due to the change of the electric potential are considered exactly. This feature enables both, rapid convergence of the Newton-Raphson method and noise analysis.

As an numerical example, the noise performance of a DG MOSFET is investigated. From the simulation results, it is confirmed that the larger part of the terminal current noise stems from the source side.

Acknowledgment

The authors gratefully acknowledge financial support by the Deutsche Forchungsgemeinschaft (DFG JU 406/6-1).

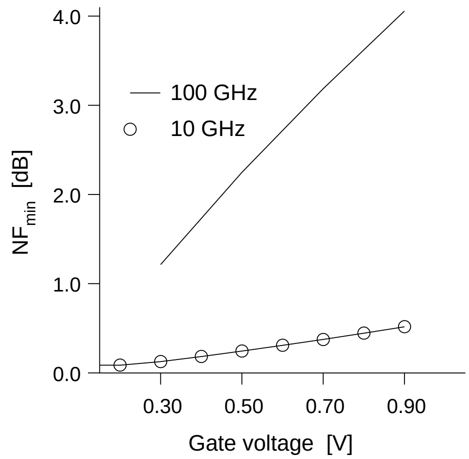

Fig. 12. Minimum noise figure as a function of V_{GS} at V_{DS} = 0.9 V and frequencies 10 and 100 GHz.

References

[1] A. Gnudi, D. Ventura, G. Baccarani, and F. Odeh, "Two-dimensional MOSFET simulation by means of a multidimensional spherical harmonics expansion of the Boltzmann transport equation," *Solid–State Electron.*, vol. 36, no. 4, pp. 575 – 581, 1993.

[2] R. Brunetti, C. Jacoboni, F. Nava, L. Reggiani, G. Bosman, and R. J. J. Zijlstra, "Diffusion coefficient of electrons in silicon," *J. Appl. Phys.*, vol. 52, pp. 6713–6722, 1981.

[3] W. Liang, N. Goldsman, I. Mayergoyz, and P. Oldiges, "2- D MOSFET modeling including surface effects and impact ionization by self-consistent solution of the Boltzmann, Poisson, and hole-continuity equations," *IEEE Trans. Electron Devices*, vol. 44, no. 2, pp. 257–267, 1997.

[4] C. Lombardi, S. Manzini, A. Saporito, and M. Vanzi, "A physical based mobility model for numerical simulation of nonplanar devices," *IEEE Trans. Computer–Aided Des.*, vol. 7, pp. 1164–1170, 1988.

[5] C. Jungemann, A.-T. Pham, B. Meinerzhagen, C. Ringhofer, and M. Bollhöfer, "Stable discretization of the Boltzmann equation based on spherical harmonics, box integration, and a maximum entropy dissipation principle," *J. Appl. Phys.*, vol. 100, pp. 024 502–1–13, 2006.

[6] C.-K. Lin, N. Goldsman, Z. Han, I. Mayergoyz, S. Yu, M. Stettler, and S. Singh, "Frequency domain analysis of the distribution function by small signal solution of the Boltzmann and Poisson equations," in *Proc. SISPAD*, 1999, pp. 39–42.

[7] C. Jungemann, "A deterministic approach to RF noise in silicon devices based on the Langevin Boltzmann equation," *IEEE Trans. Electron Devices*, vol. 54, no. 5, pp. 1185–1192, 2007.

[8] C. Jungemann, B. Neinhüs, C. D. Nguyen, A. J. Scholten, L. F. Tiemeijer, and B. Meinerzhagen, "Numerical modeling of RF noise in scaled MOS devices," *Solid–State Electron.*, vol. 50, pp. 10–17, 2006.

[9] F. M. Klaassen and J. Prins, "Thermal noise of MOS transistors," *Philips Res. Repts*, pp. 505–514, 1967.

[10] R. Rengel, M. J. Martin, T. Gonzalez, J. Mateos, D. Pardo, G. Dambrine, J.-P. Raskin, and F. Danneville, "A microscopic interpretation of the RF noise performance of fabricated FDSOI MOSFETs," *IEEE Trans. Electron Devices*, vol. 53, no. 3, pp. 523 – 532, 2006.

[11] A. van der Ziel, *Noise in Solid State Devices and Circuits*. Canada: John Wiley and Sons, 1986.